HIGH PRECISION RF CONTROL FOR THE LCLS-II*

G. Huang†, K. Campbell, L. Doolittle, Q. Du, J. Jones,
C. Serrano, V. Vytla, LBNL, Berkeley, CA 94720, USA
S. Babel, M. Boyes, G. Brown, D. Cha, G. Dalit, J. DeLong, B. Hong, A. McCollough,
A. Ratti, C. Rivetta, SLAC, Menlo Park, CA 94720, USA
R. Bachimanchi, C. Hovater, D. Klepec, D. Seidman, JLAB, Newport News, VA 23606, USA
B. Chase, E. Cullerton, J. Einstein-Curtis, O. Kumar, FNAL, Batavia, IL 60555, USA

ABSTRACT

The LCLS-II is a CW superconducting linac under construction to drive an X-ray FEL. The energy and timing stability requirements of the FEL drive the need for very high precision RF control. This paper summarizes the design considerations and early demonstration of the performance of the modules and system we developed.

INTRODUCTION

LCLS-II is a project to generate high quality, high repetition rate soft X-ray beam for advanced science discovery. The project will construct a 4 GeV superconducting linac in the existing SLAC tunnel. The accelerated electrons will be sent through undulators to produce X-rays.

LCLS-II requires electron beam jitter and energy spread better then 20 fs and 0.014% at the undulator to achieve its X-ray beam quality goals. That, in turn, requires 0.01° in phase and 0.01% amplitude stability for the RF field in each superconducting 1300 MHz cavity. [1]

The superconducting linac will contain 35 cryomodules, each with eight 9-cell 1.3 GHz superconducting cavities. The machine layout is shown in Figure 1.

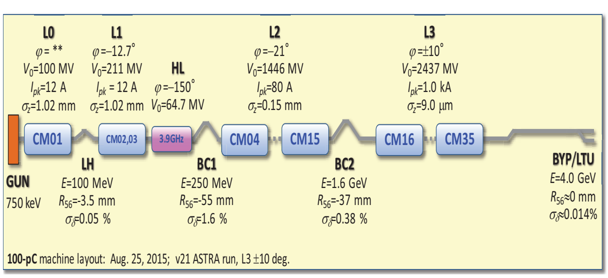

Figure 1: LCLS-II Linac layout.

A system design is a compromise of different parameters, including cost, robustness, noise *etc.* Series of project architectural choices made the high precision RF control possible for the machine. The low level RF collaboration team designed the low noise digital LLRF system to minimize the noise sources within the control bandwidth. Noise or disturbances outside the LLRF system's control bandwidth must be either handled by a beam-based feedback system or be eliminated from the source. [2–4]

SYSTEM ARCHITECTURE SELECTION

Digital Low Level RF Control System

The low level RF control system measures the cavity pickup signal and compares it with the vector set point to generate an error signal. The error signal goes through a Proportional and Integral control loop and generates the correction to drive the high power RF system. With the development of ADC, DAC and FPGA technology, the system can be implemented digitally as shown in Figure 2. The flexibility and self-monitoring capability of a digital implementation is so advantageous that analog systems are no longer considered.

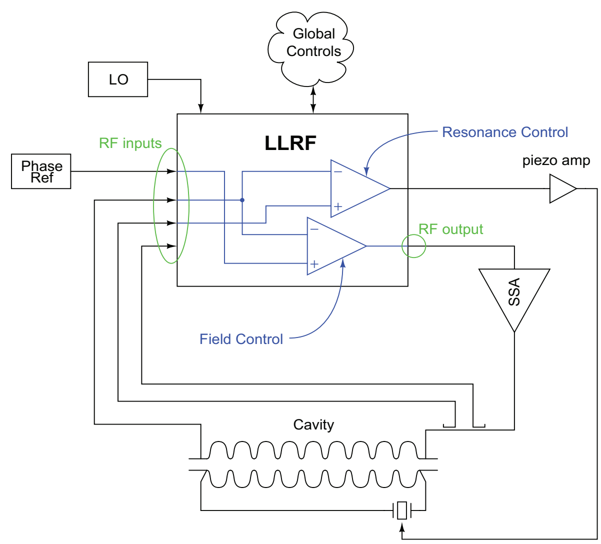

Figure 2: Abstract LLRF feedback topology.

Single Source Single Cavity

In the LCLS-II, the linac RF will run in CW mode with high loaded Q. It will be more sensitive to microphonics than pulsed machines. Unlike pulsed machines, the Lorentz Force Detuning effect is static once the amplitude of each cavity is stabilized with feedback.

A single-source single-cavity configuration is selected to give each cavity its own low level RF system. Thus it can combine the piezo and RF power to fight against microphonics. During turn on or recovery from a fault, the system will use Self Excited Loop mode, which is by construction free of ponderomotive instability.

* Work supported by the LCLS-II Project and the U.S. Department of Energy, Contract DE-AC02-76SF00515
† ghuang@lbl.gov

Phase Reference Line

The cavities in the beginning sections (L0, L1, L2) of the linac are designed to run off-crest, leading to strong machine sensitivity to cavity phase errors. The phase reference must be distributed to each cavity with high precision, and LLRF for each cavity will regulate the cavity field phase relative to the distributed phase reference.

A hard coaxial line phase reference distribution system based on the concept shown in Figure 3 is chosen. This concept has been field-proven with analog designs at SLAC and FNAL. [5] Slow, temperature-induced changes in the electrical length of all parts of the coaxial line will be compensated in the average phase of the forward and reverse signal phase. In this project, we will do the averaging digitally.

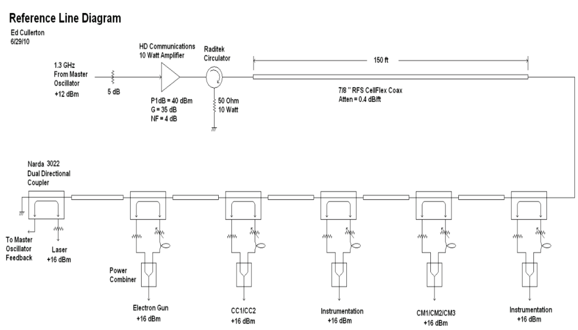

Figure 3: Concept of phase reference line.

Beam Based Feedback

The LLRF system can hold the amplitude of each cavity relative to its amplitude reference, but the absolute amplitude of each cavity is hard to characterize. A slow beam-based feedback system is planned to correct any drift in the control system hardware. Such a system can also correct long-term imperfections of the phase reference line. A fast beam based feedback system could in theory be added to increase this correction bandwidth, but is left out of the project baseline as of now.

SYSTEM MODELING

In order to better understand the system behavior, we developed a RF control system simulation code and an accelerator end-to-end simulation code.

A superconducting cavity model with multiple mechanical oscillation modes and multiple electromagnetic modes and the coupling among them is developed and used in both codes. The block diagram of the the cavity model is shown in Figure 4.

The RF control system simulation code is designed to run on a FPGA directly, so we called the CryoModule On Chip (CMOC). The CMOC simulation can run in real time, much faster than achievable with software simulation. So it can help us model the microphonics and develop low level RF control algorithm. Such a model can also be used to develop

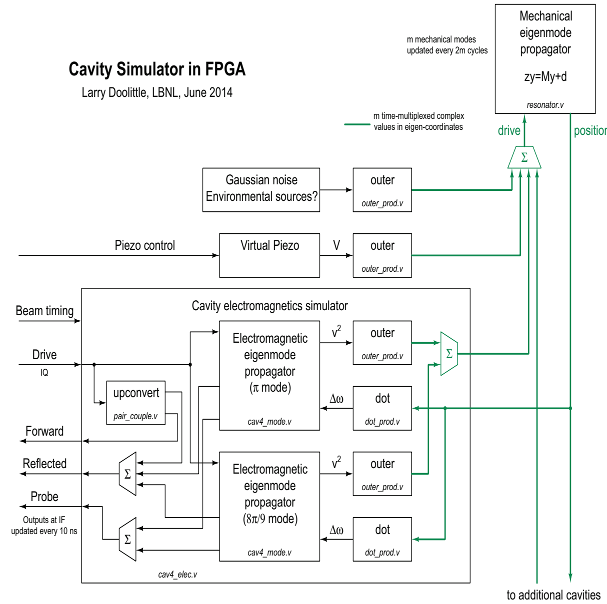

Figure 4: Cavity model simulator block diagram.

high level software, long before cryomodules are available for testing.

The accelerator end-to-end simulation code contains the macro-particle beam dynamic model, so it is used to analyze the system transfer function and noise propagation. [6, 7]

SYSTEM DESIGN

Network Attached Device

A low level RF system can be packaged in many different form factors. We chose to develop stand-alone chassis and communicate via a network, which gets labeled a Network Attached Device (NAD) or pizza-box. Compared with many industrial standards, like VXI, VME, μTCA, ATCA, a NAD can engineer in clean solutions to EMC/EMI and thermal stability issues, in part because of a lack of artificial space constraints.

RF Station and Precision Receiver Chassis

For a feedback loop as shown in Figure 2, the in-band noise from the receiver side will be added to the cavity field noise, and the noise from the amplifier will be suppressed by the feedback gain. So as usual, the receiver noise will be critical for the system performance. The RF signal from cavity forward and reverse waves can couple into the feedback receiver chain, which will also add error to the cavity field.

The critical signals for feedback accuracy are four cavity probe signals and two phase reference signals; these are acquired in a Precision Receiver Chassis (PRC), as shown in Figure 5. The PRC is placed in the rack's best temperature controlled area. The phase error is calculated in the PRC chassis and sent to the RF Station (RFS) chassis in the digital domain over fiber. The remaining RF signals acquired by the RFS chassis are less critical for cavity field stability, so its ambient temperature control needs are less stringent. The

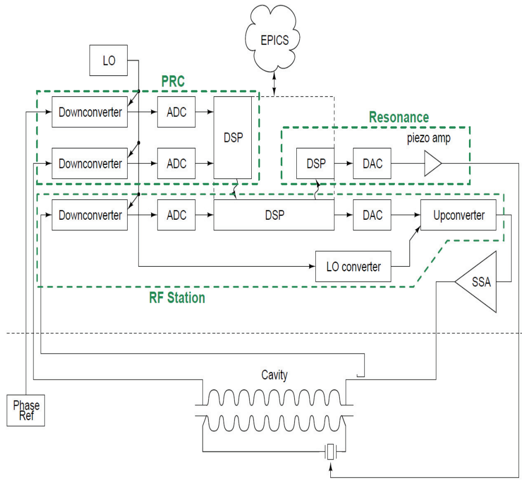

Figure 5: Simplified RF Architecture.

PI field-control loop and the RF drive will be implemented in the RFS chassis.

This separation of chassis has some clear advantages:

- It keeps microphonically varying forward and reverse RF signals away from the critical probe RF;
- It digitally duplicates the reference digitizer result across four stations;
- It keeps the most sensitive measurements away from most sources of EMI.

Active Resonance Control

The cavity resonance frequency is constantly changing due to external microphonics and helium pressure drift. When the cavity characteristic frequency is different from the nominal frequency, the system will use extra power to achieve constant acceleration gradient. An active resonance control system is designed to tune the cavity to ±0.5 Hz on average, with allowance for dynamic excursions of ±10 Hz. A block diagram of the LCLS-II LLRF is shown in Figure 6.

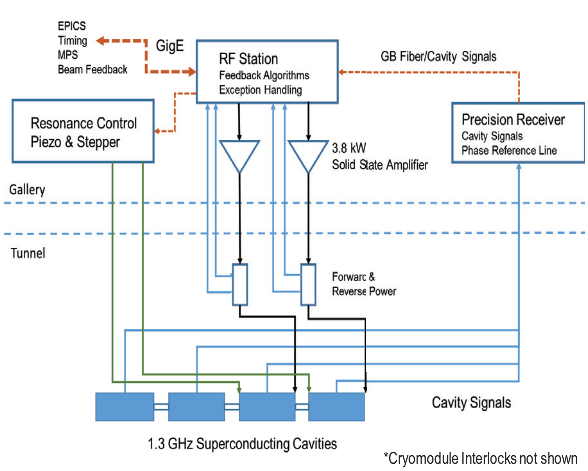

Figure 6: LLRF Architecture.

Up and Down LO Frequency

Another potential path for crosstalk between the transmitter and the receiver is the Local Oscillator, especially when a single distribution amplifier supplies both the up converter and down converter. We chose to separate the up and down converter LO frequency to minimize the cross talk.

Thermal Design

The LCLS-II LLRF system rack will be placed in the SLAC gallery, where the day/night, summer/winter temperature excursions can go up to 35° C. We have engineered a set of thermal techniques to keep the RF performance stable in spite of the harsh environment.

The rack itself will be crudely sealed from outside air. Fans will circulate air through the chassis and a heat-exchanger, to extract the ~250 W dissipated within the rack.

Each RF chassis has cooling air separated from its active components by a 6 mm thick aluminum plate, which acts as a thermal low-pass filter. The airspace with cables and analog components is "dead," without turbulence that can create instability in the measurements. RF and analog circuit boards are thermally connected to the plate with 0.5 mm thick thermal-conductive foam, and thus are designed without back-side components.

Group Delay

The field control feedback group delay is budgeted in Table 1. The 2000 ns total delay can sustain 40 kHz closed loop bandwidth.

Table 1: LLRF Group Delay Budget

(ns)	Description
50	Input analog BPF
170	ADC pipe (16 cycles at 94.3 MHz)
64	Precision Rx DSP (12 cycles at 188.6 MHz)
140	GTP and fiber latency
106	Controller DSP (20 cycles at 188.6 MHz)
1000	Bandpass filter in DSP (200 kHz)
70	Notch filter in DSP (~800 kHz for $8\pi/9$ mode)
40	DAC (7 cycles at 188.6 MS/s)
20	Sideband selection filter
170	Estimated SSA
100	Cables and waveguides
70	Contingency
2000	Total

Frequencies in the LLRF System

The key frequencies and their relationship in the LLRF system are summarized in the Table 2. The system repeat period is 1.4 μs; including the LCLS-I system, the repeat period is 14 μs. [8]

MODULES DEVELOPMENT AND TEST

The hardware modules of the LCLS-II LLRF prototype system were built in different laboratories, and assembled

Table 2: LCLS-II SC LLRF Frequencies

	MHz	
f_{RF}	1300	
f_{LO}	1320	$f_{RF} \cdot 66/65$
f_{PRL}	1300	f_{RF}
f_{ADCCLK}	94.3	$f_{LO}/14$
f_{DACCLK}	188.6	$f_{LO}/7$
f_{LOdn}	1320	f_{LO}
f_{IFdn}	20	$f_{RF} - f_{LOdn} = f_{ADCCLK} \cdot 7/33$
f_{LOup}	1155	$f_{LO} - f_{LO}/8$
f_{IFup}	145	$f_{RF} - f_{LOup} = f_{ADCCLK} \cdot 203/132$

into chassis as shown in Figure 6. Figure 7 shows a picture of the RFS chassis, which integrated the frequency up converter, the frequency down converter, the digitizer board, the digital board, and the power distribution board. The

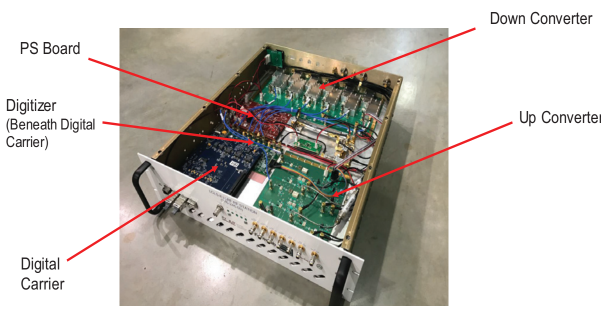

Figure 7: LCLS-II LLRF RF station.

PRC chassis shares most of its design with the RFS chassis, except it does not have the up converter board and associated circuits. The resonance control chassis uses the same digital board, along with stepper motor drives and low-noise high-resolution analog outputs for the piezoelectric actuators. Chassis communicate to each other via fiber link through the QSFP modules on the digital carrier board.

Low Noise Frequency Down Converter

The 1.3 GHz RF signal is mixed with the distributed Local Oscillator and low pass filtered to generate an Intermediate Frequency (IF) signal which can be digitized. Both noise and crosstalk between channels will contribute to receiver measurement errors.

A low noise 6-channel down converter board was developed at FNAL as shown in Figure 8. The board uses a Mini-Circuits SYM-25DMHW+ level 13 mixer. The board is directly mounted to the chassis rear panel, to eliminate extra cable and connectors in the critical input path. Each channel gets its own power regulator to minimize the crosstalk through power supply lines. Surface mounted connectors and components together with the via fence confine the signal to a single layer. Aluminum covers enclose each channel to improve isolation. Bench tests show the board achieves >87 dB channel-to-channel isolation and <-157.7 dBm/$\sqrt{\text{Hz}}$ output noise.

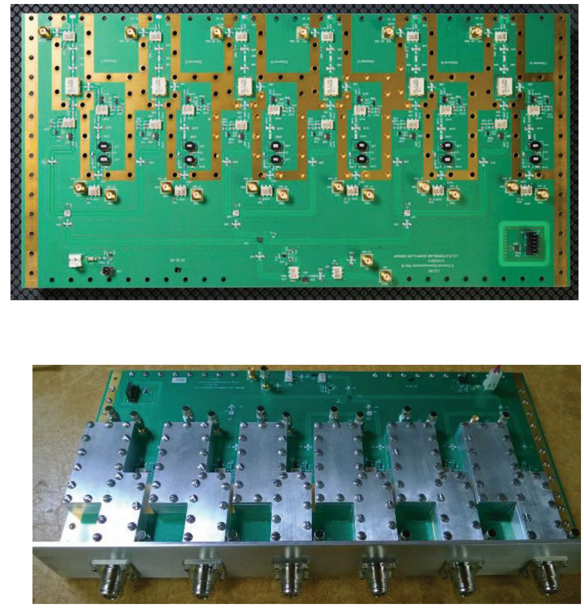

Figure 8: LCLS-II LLRF 1.3 GHz 6-Channel down converter.

Low Noise Digitizer

The down converted IF signal from cavity probes and the phase reference line signals are digitized with a board developed at LBNL as shown in Figure 9. The digitizer board is designed to synchronously convert up to 8 IF signals to digital; it also can provide two channels of DAC output (used in the RF Stations) as well as extra digital pins. [9]

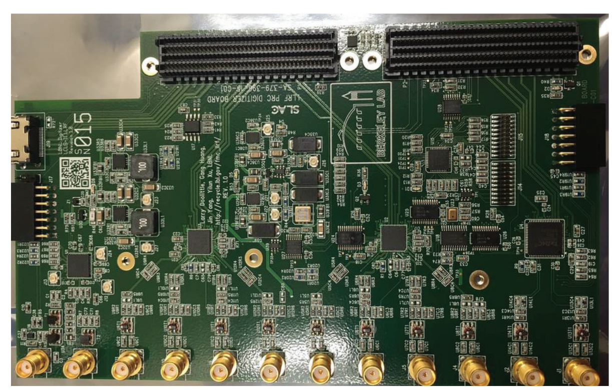

Figure 9: LCLS-II LLRF digitizer board

The system local oscillator is divided down by a clock divider buffer (LMK01801) to provide clocks for ADCs and DAC. The AD9653 ADC from Analog Devices was chosen for its 77.5 dB signal to noise ratio, and because it only requires 5 FPGA pins per channel.

Bench tests show the board achieve >80 dB channel-to-channel isolation and <-151 dBc/$\sqrt{\text{Hz}}$ additive phase noise.

FPGA Processing Algorithm

DSP in the FPGAs implements all the required functionality of the system; the analog electronics serve as I/O for the

FPGA. The Field Control feedback loop uses two FPGAs (PRC and RFS), and a high-speed (4 Gbaud) fiber link between them. The Resonance Control feedback loop also uses two FPGAs (RFS and Resonance), and another fiber link between them. In a sense we use the set of fiber communication paths the same way previous decades used a Eurocrate backplane; except with checksums, signal strength monitoring, and zero EMI.

We have coded, and tested in simulation, the main Field Control loop based on Self-Excited loop concepts [10] that have proven themselves suitable for the narrow-band, microphonics-stressed, strong-Lorentz-detuning CW SRF environment.

Figure 10: LLRF Testing at the FNAL CMTS.

Initial Test Setup in FNAL CMTS

LCLS-II project built a prototype CryoModule (pCM) and is testing its performance in FNAL; a similar pCM will also be tested at JLAB. The cryomodule characterization will use the existing RF controller in each laboratory, but these pCM tests also give the LLRF collaboration team a chance to test the new hardware and system with the cold cavity. These tests are facilitated by splitting a set of cavity probe, forward and reverse signals for the two systems. Actually driving the SSA and cavity requires swapping just one cable per cavity.

Test plans are in-place to exercise the system and measure its performance. [11]

Figure 10 shows the chassis as installed in FNAL's CryoModule Test Station (CMTS), which includes the power supply, PRC, RFS, and resonance control chassis. A fan is installed on the top of the rack, and the rack is coarsely sealed, to force air through each of the chassis for cooling.

We have started to collect some initial data to calculate the cavity loaded Q_L, measure microphonics of that environment, and characterize SSA linearity.

SUMMARY

High precision RF control of the accelerator cavity field is required for the LCLS-II project. A series of architecture choices have been made by the project, making it possible to develop a high precision RF control system. A collaboration team of LLRF experts from four laboratories designed the LLRF system with value engineering in mind. A prototype of the system has been developed and bench tested with state-of-the-art performance. The integrated system will be tested on the project's prototype CryoModule.

REFERENCES

[1] P. Emma, "LCLS-II Physics Requirement Document: Linac Requirements," LCLSII-2.4-PR-0041-R2.

[2] C. Hovater, L. Doolittle, "The LCLS-II LLRF System" in *Proceeding of IPAC2015*, Richmond, VA, USA, 2015.

[3] L. Doolittle, A. Ratti *et al.*, "Design of RF Controls for Precision CW SRF Light Sources," in *Low Level RF workshop 2013*, Lake Tahoe, CA, October 2013.

[4] L. Doolittle, "Analog-centered LLRF System Design for LCLS-II," in *Low Level RF workshop 2015*, Shanghai, China, October 2015.

[5] E. Cullerton, B. Chase., "1.3 GHz Phase Averaging Reference Line" in *Low Level RF workshop 2013*, Lake Tahoe, CA, October 2013.

[6] C. Serrano, L. Doolittle, "LLRF Control of High Q_L Cavities for the LCLS-II," in *Proceedings of IPAC2016*, Busan, Korea, 2016.

[7] "End-to-end FEL beam stability simulation engine" in *Proceedings of IPAC2016*, Busan, Korea, 2016.

[8] L. Doolittle, H. Ma, "Digital low-level RF control using non-IQ sampling" in *Proceedings of LINAC2006*, Knoxville, TN, August 2006.

[9] G. Huang, L. Doolittle *et al.*, "Low noise digitizer design for LCLS-II LLRF" presented at NAPAC2016, Chicago, IL, October 2016, this conference.

[10] J. R. Delayen, "Phase and Amplitude Stabilization of Superconducting Resonators," Ph.D Thesis, Caltech, 1978.

[11] C. Hovater, "LLRF Controls" LCLS-II DOE Review, Oct. 2016.